



Análisis de una célula solar de silicio BC-BJ de contacto puntual mediante simulaciones numéricas tridimensionales

Analysis of a point-contact BC-BJ silicon solar cell by three-dimensional numerical simulations

Análise de uma célula solar de silício BC-BJ de ponto de contato por meio de simulações numéricas tridimensionais

Esteban Augusto Guevara-Cabezas¹
esteban.guevara@espoch.edu.ec
<https://orcid.org/0000-0001-6652-047X>

Correspondencia: esteban.guevara@espoch.edu.ec

Ciencias Técnicas y Aplicadas
Artículo de Revisión

*Recibido: 30 de Agosto de 2020 *Aceptado: 22 de Septiembre de 2021 * Publicado: 12 de Octubre de 2021

- I. Médica Laurea Magistrale in Ingegneria Elettronica, Laurea in Ingegneria Elettronica, Escuela Superior Politécnica de Chimborazo ESPOCH, Riobamba, Ecuador.

Resumen

El diseño de células solares optimizadas y eficientes es un factor clave para el desarrollo futuro de la tecnología fotovoltaica (PV). Este artículo se centra en el modelado tridimensional (3D) de células solares de silicio cristalino (c-Si) de unión trasera-contacto posterior (BC-BJ) que presentan un esquema de contacto puntual (PC) en la región del emisor trasero para optimizar la eficiencia con respecto al uso de un patrón de contacto lineal convencional (LC). Se ha construido un modelo 3D para garantizar una buena precisión en la simulación de las estructuras de células solares consideradas. El modelo desarrollado incluye un modelado adecuado de los efectos de resistencia en serie relacionados con el patrón de contacto implementado. El software TCAD Sentaurus proporcionado por Synopsys ha sido adoptado para realizar simulaciones comparativas entre la celda solar PC BC-BJ considerada y su contraparte LC. Los resultados de nuestra simulación demuestran que la adopción de un esquema de PC en la región emisora de una celda solar BC-BJ es beneficiosa para aumentar su eficiencia (hasta un 22,43%) con respecto a la celda LC convencional, mientras mantiene más baja la fracción en contacto de la región emisora.

Abstract

The design of optimized and efficient solar cells is a key factor for the future development of the photovoltaic (PV) technology. This paper focuses on three-dimensional (3D) modeling of a Back Contact-Back Junction (BC-BJ) crystalline silicon (c-Si) solar cells featuring a point contact (PC) scheme in the rear emitter region in order to optimize the efficiency with respect to the use of a conventional linear contact (LC) pattern. A 3D model has been built to ensure a good accuracy in the simulation of the considered solar cell structures. The developed model includes a proper modeling of the series resistance effects related to the implemented contact pattern. The TCAD Sentaurus software provided by Synopsys has been adopted to perform comparative simulations between the considered PC BC-BJ solar cell and its LC counterpart. Our simulation results prove that the adoption of a PC scheme in the emitter region of a BC-BJ solar cell is beneficial to boost its efficiency (up to 22.43%) with respect to the conventional LC cell, while keeping lower the contacted fraction of the emitter region.

Resumo

O design de células solares otimizadas e eficientes é um fator chave para o futuro desenvolvimento da tecnologia fotovoltaica (PV). Este artigo se concentra na modelagem tridimensional (3D) de células solares de silício cristalino (c-Si) de junção de contato traseiro (BC-BJ) apresentando um esquema de contato de ponto (PC) na região emissora traseira, a fim de otimizar o eficiência no que diz respeito ao uso de um padrão convencional de contato linear (LC). Um modelo 3D foi construído para garantir uma boa precisão na simulação das estruturas de células solares consideradas. O modelo desenvolvido inclui uma modelagem adequada dos efeitos de resistência em série relacionados ao padrão de contato implementado. O software TCAD Sentaurus fornecido pela Synopsys foi adotado para realizar simulações comparativas entre a célula solar considerada PC BC-BJ e sua contraparte LC. Nossos resultados de simulação comprovam que a adoção de um esquema de PC na região emissora de uma célula solar BC-BJ é benéfica para aumentar sua eficiência (até 22,43%) em relação à célula LC convencional, enquanto mantém baixa a fração de contato do região emissora.

Introduction

Solar cells are typically fabricated using semiconductor materials, most commonly crystalline silicon, polycrystalline silicon, and amorphous silicon. However, GaAs, GaInP, Cu(InGa)Se₂, and CdTe can be also used for solar cells. These materials are mostly chosen on their absorption characteristics of the solar spectrum and their fabrication cost. Crystalline silicon (c-Si) represents the usual choice since its absorption characteristics are a fairly good match to the solar spectrum, and c-Si fabrication technology is well developed as a result of its pervasiveness in the semiconductor electronics industry. As a matter of fact, c-Si solar cells currently dominate the photovoltaic (PV) market [1].

In this context, one of the goals of researchers working in the PV field is to study and develop more advanced solar cell architectures aimed at improving the conversion efficiency. Back Contact-Back Junction (BC-BJ) solar cells, also called Interdigitated Back Contact (IBC) solar cells, represent a promising concept to obtain high efficiencies [2]-[9], also exceeding 24% [6]. In these cells, both emitter and base contacts/junctions are placed at the rear side in the form of an interdigitated grid. This allows avoiding optical shadowing losses at the front side, and

simplifying the interconnection process at the module level. However, BC-BJ solar cells typically require high lifetime in the silicon substrate and very good front and rear surface passivation to minimize recombination losses within the device [4]. Moreover, an optimized design of the rear contact geometry is fundamental to maximize the efficiency of BC-BJ solar cells [5]-[9]. In this regard, this work focuses on the study of a BC-BJ solar cell featuring a point contact (PC) scheme [5]-[9] in the rear emitter region as compared to a conventional BC-BJ cell with a linear contact (LC) pattern [2]-[4]. To perform such comparative analysis, a three-dimensional (3D) electro-optical TCAD model has been developed in the Synopsys Sentaurus simulator [10]. Note that a 3D modeling approach is mandatory when dealing with point contact solar cells to account for all the physical mechanisms occurring in the device, such as recombination and series resistance losses [11]. In particular, series resistance losses related to the adopted contact scheme are properly described by means of a distributed resistance model.

The rest of the paper is organized as follows. Section 2 describes in details the developed model for the considered solar cell. Section 3 reports and discusses the obtained simulation results. Finally, Section 4 draws the main conclusions of our work.

Modeling of the BC-BJ solar cell

Fig. 1 shows the two-dimensional (2D) cross-section of the simulated solar cell based on a c-Si n-type substrate. The same figure illustrates the symmetry element of the cell corresponding to its simulation domain, whose width is half of the rear contact pitch [4].

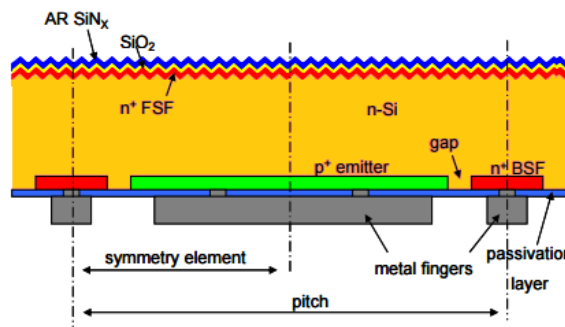


Fig. 1. Cross-section of the Back Contact-Back Junction (BC-BJ) silicon solar cell.

The front side is covered by a double $\text{SiN}_x/\text{SiO}_2$ anti-reflective coating (ARC) layer to reduce reflection and recombination losses and it features an n^+ -type front surface field (FSF) to reduce

the concentration of the minority carriers at the front surface, thus minimizing the front surface recombination losses [4]. At the rear side, the solar cell features n^+ -type back surface field (BSF) and p^+ -type emitter regions in correspondence of base and emitter metal fingers, respectively, with an emitter-BSF spacing gap, while the non-contacted rear side areas are passivated by a SiO_2 layer.

Fig. 2 highlights the main geometrical parameters of the simulated solar cell. Among these, D_{sub} is the thickness of the silicon substrate, $D_{\text{Oxide}F}$ is the thickness of the $\text{SiN}_x/\text{SiO}_2$ front ARC layers, W_{BSF} is the width of the BSF region, W_{emitt} is the width of the emitter region, W_{contBSF} is the width of the BSF metal contact, and $W_{\text{contemitt}}$ is the width of the emitter metal contact.

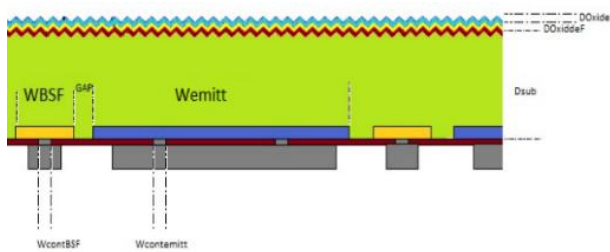


Fig. 2. Main geometrical parameters in the simulated BC-BJ solar cell.

Fig. 3 shows the 3D geometrical model of the simulated BC-BJ solar cell. It features a LC scheme in the rear BSF region, while in the rear emitter region a PC scheme consisting of an array of localized metal points that contact the silicon via small openings is adopted [9]. For the sake of comparison, we have also simulated a conventional BC-BJ solar cell with a LC scheme in both BSF and emitter regions at the rear side.

To perform accurate electrical simulations in the TCAD simulator, the use of a proper mesh is required [10]. In this regard, Fig. 4 shows the developed mesh for the simulated BC-BJ solar cell. It is worth pointing out that a mesh refinement is fundamental close to the front surface where most of the incident photons are absorbed, at the FSF, BSF, and emitter junctions, and around the contacts at the rear side. Electrical simulations of the two considered solar cells have been carried out by using the drift-diffusion model, while enabling Fermi-Dirac statistics to accurately model the highly doped regions [4]. A proper refinement of the physical models and parameters included in the TCAD simulator has been done considering more recent parameterizations proposed in literature [12]-[14]. In addition, the 3D map of the optical generation within the device has been

developed by interpolating on the 3D mesh adopted for the electrical simulations (see Fig. 4) two different one-dimensional (1D) profiles of the optical generation rate corresponding to rear non-contacted (i.e. passivated) and contacted areas, respectively. These 1D optical profiles have been obtained from 3D optical simulations based on ray tracing methodology, while taking into account the effect of the texturing at the front side [4].

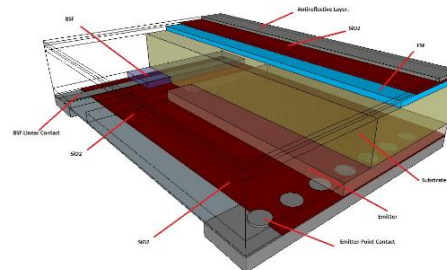


Fig. 3. 3D model of the simulated BC-BJ solar cell with a linear contact (LC) scheme in the BSF region and a point contact (PC) scheme in the emitter region.

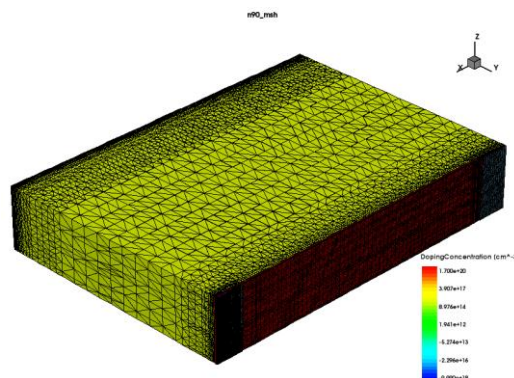


Fig. 4. Detail of the mesh developed for the simulated solar cell.

To model the series resistance effects related to the contributions of contact and metal finger resistances at the rear side, we have adopted a distributed resistance model, as shown in Fig. 5(a)-(b) for the BC-BJ solar cell featuring a LC scheme in the BSF region and a PC scheme in the emitter region. Note that, for the sake of simplicity, rear point contacts with rectangular shape have been considered.

The contact resistance (defined by the parameter Resist in the adopted TCAD simulator [10]) in the BSF region has been modeled according to the following equation

$$Resist_{BSF} = \frac{1}{2} \frac{\rho_c}{W_{contBSF}} * \frac{Depth}{2} \quad (1)$$

where ρ_c is the contact resistivity at the rear contacted interfaces, and *Depth* is the length of the linear contact in the simulated solar cell, thus corresponding to the depth of the considered simulation domain. Note that, in (1), the contact resistance is modeled considering the metal finger composed of two parallel metals, each with a width equal to $W_{contBSF}/2$. This allows accounting for the current coming from both sides of the metal finger. Therefore, we have introduced a factor 1/2 in (1) according to the parallel of two identical resistances [15].

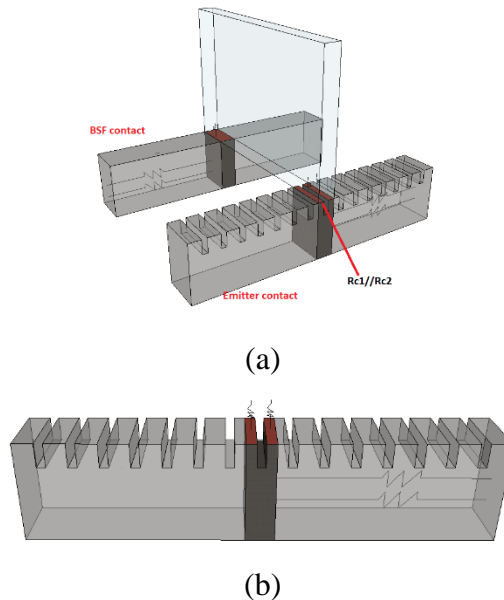


Fig. 5. Resistance model for the simulated BC-BJ solar cells with a LC scheme in the BSF region and a PC scheme in the emitter region: (a) 3D sketch of BSF and emitter metal contacts, and (b) detail of the emitter PC model.

Conversely, the contact resistance associated to point contacts in the emitter region has been modeled as

$$Resist_{emitt} = \frac{1}{2} \frac{\rho_c}{W_{contemitt}} * \frac{Depth}{2} * F \quad (2)$$

where F is a factor that accounts for the PC pattern, defined as

$$F = \frac{Depth_{PC}}{Depth} \quad (3)$$

i.e. the ratio of the depth of the rectangular point contacts (DepthPC) to the total depth of the simulated cell.

Moreover, the distributed metal finger resistance in both BSF and emitter regions has been described by properly defining the DistResist parameter in the developed TCAD model [10], as given by

$$DistResist = \frac{1}{3} \rho_m \frac{L^2}{t_c * Depth} \quad (4)$$

where ρ_m is the metal resistivity, L is the whole finger length, Depth is the finger length in the simulated device (corresponding to the depth of the simulation domain, as stated above), and t_c is the finger thickness.

Simulation results

The effect of the PC scheme adopted in the emitter region has been evaluated by varying the rear emitter contact fraction (CFemitt), i.e. the ratio of the contacted area in the emitter region to the total emitter area (considering Wemitt = 400 μm). The CFemitt has been changed by varying the DepthPC of the rectangular point contacts, while keeping constant the Wcontemitt at 18 μm and the pitch between two adjacent point contacts. Simulation results of the considered BC-BJ cell with a PC scheme in the emitter region have been compared with those obtained for the BC-BJ cell featuring a LC scheme in both BSF and emitter regions. The latter has a fixed CFemitt = 4.5%, which corresponds to its optimal value with Wcontemitt = 18 μm .

Fig. 6 shows obtained results in terms of short circuit current density (J_{sc}) versus CFemitt for the simulated PC solar cell.

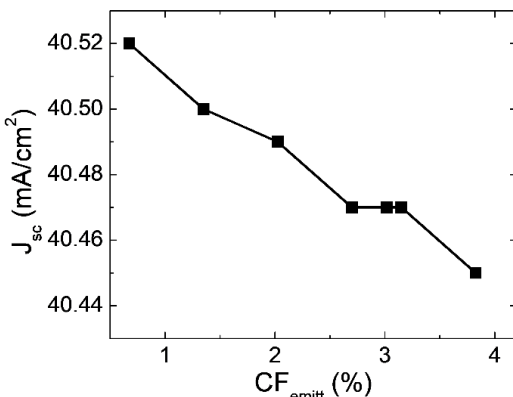


Fig. 6. Short circuit current density (J_{sc}) versus CF_{emitt} for the simulated PC solar cell.

From Fig. 6 we can note that the J_{sc} tends to decrease for increasing CF_{emitt} due to the increase of surface recombination losses at the rear-side contacted interface [11]. For the same reason, the open circuit voltage (V_{oc}) exhibits a similar trend, as shown in Fig. 7.

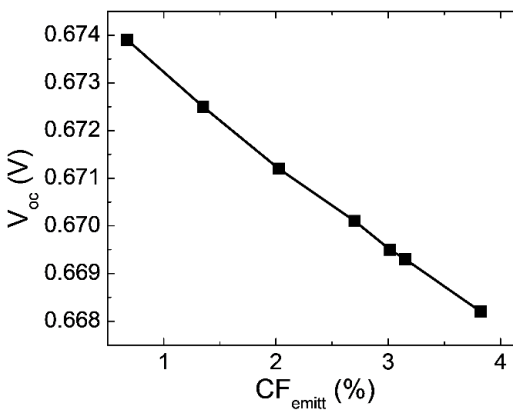


Fig. 7. Open circuit voltage (V_{oc}) versus CF_{emitt} for the simulated PC solar cell.

Fig. 8 shows fill factor (FF) results versus CF_{emitt} for the simulated PC solar cell.

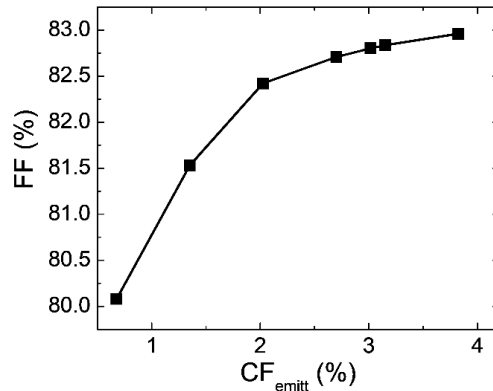


Fig. 8. Fill factor (FF) versus CF_{emitt} for the simulated PC solar cell.

As shown in Fig. 8, the FF exhibits an opposite trend with the CF_{emitt} as compared to the J_{sc} and V_{oc}. This because, when increasing the CF_{emitt}, series resistance losses related to the rear metal contacts and the lateral carrier transport inside the device decrease [11], thus resulting into an improved FF.

Fig. 9 illustrates the results in terms of conversion efficiency (η) as a function of the CF_{emitt} for the simulated PC solar cell, along with the η obtained for the LC cell with fixed CF_{emitt} = 4.5%.

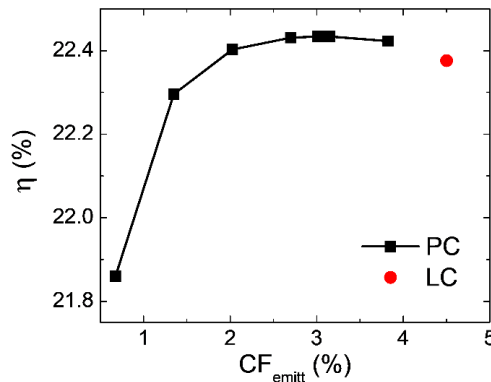


Fig. 9. Conversion efficiency (η) versus CF_{emitt} for the simulated PC solar cell, along with the η obtained for the LC cell with fixed $CF_{emitt} = 4.5\%$.

As a result of the J_{sc} and V_{oc} decreasing trend (see Fig. 6 and 7) and the FF increasing trend (see Fig. 8) with the CF_{emitt} , the efficiency curve of the PC solar cell exhibits a bell shape with a maximum value equal to $\eta_{max} \approx 22.43\%$ at an optimal $CF_{emitt} \approx 3.1\%$. As shown in Fig. 9, such efficiency is higher than that of the conventional LC cell with optimal $CF_{emitt} = 4.5\%$. This demonstrates that the adoption of the PC scheme in the emitter region of a BC-BJ solar cell is beneficial to boost the cell efficiency, while using a lower CF_{emitt} with respect to the conventional LC cell.

Finally, Table 1 summarizes the simulation results corresponding to the optimized designs of the emitter contact pattern for the two simulated BC-BJ solar cells.

Table 1. Summary results for the simulated PC and LC solar cells.

W_{emitt} [μm]	$W_{contemitt}$ [μm]	CF_{emitt} [%]	J_{sc} [mA/cm ²]	V_{oc} [mV]	FF [%]	η [%]
LC solar cell						
400	18	4.5	40.48	667.2	82.84	22.37
PC solar cell						
400	18	3.1	40.47	669.5	82.80	22.43

Conclusions

In this work, a Back Contact-Back Junction (BC-BJ) c-Si solar cell with a point contact (PC) scheme in the rear emitter region has been evaluated against its conventional counterpart featuring a linear contact (LC) scheme. To perform such comparative analysis, a three-dimensional (3D) electro-optical TCAD model developed in the Synopsys Sentaurus simulator has been exploited. Obtained simulation results prove that the PC solar cell reaches a higher efficiency (up to 22.43%) with respect to the conventional LC cell, while keeping lower the contacted fraction of the emitter region.

References

1. D. A. Neamen. *Semiconductor Physics and Devices: Basic Principles*. McGraw-Hill, 2013.
2. P. Procel et al. Numerical simulation of the impact of design parameters on the performance of back-contact back-junction solar cell. *Journal of Computational Electronics*, vol. 15, pp. 260–268, 2016.
3. M. Guevara et al. Design guidelines for a metallization scheme with multiple-emitter contact lines in BC-BJ solar cells. *Journal of Computational Electronics*, vol. 15, pp. 1498–1504, 2016.
4. P. Procel et al. Opto-electrical modelling and optimization study of a novel IBC c-Si solar cell. *Progress in Photovoltaics: Research and Applications*, vol. 25, no. 6, pp. 452–469, 2017.
5. P. Ortega et al. High-efficiency black silicon interdigitated back contacted solar cells on p-type and n-type c-Si substrates. *Progress in Photovoltaics: Research and Applications*, vol. 23, no. 11, pp. 1448–1457, 2015.
6. E. Franklin et al. Design, fabrication and characterisation of a 24.4% efficient interdigitated back contact solar cell. *Progress in Photovoltaics: Research and Applications*, vol. 24, no. 4, pp. 411–427, 2016.
7. D. Carrió et al. Rear contact pattern optimization based on 3D simulations for IBC solar cells with point-like doped contacts. *Energy Procedia*, vol. 55, pp. 47–52, 2014.

8. Zanuccoli et al. Analysis of the impact of geometrical and technological parameters on recombination losses in interdigitated back-contact solar cells. *Solar Energy*, vol. 116, pp. 37–44, 2015.
9. N. Guerra et al. Understanding the impact of point-contact scheme and selective emitter in a c-Si BC-BJ solar cell by full 3D numerical simulations. *Solar Energy*, vol. 155, pp. 1443–1450, 2017.
10. Synopsys. Sentaurus TCAD Industry-Standard Process and Device Simulators. [Online] <http://www.synopsys.com/>.
11. M. Zanuccoli et al. Performance analysis of rear point contact solar cells by three-dimensional numerical simulation. *IEEE Transactions on Electron Devices*, vol. 59, no. 5, pp. 1311–1319, 2012.
12. P. P. Altermatt. Models for numerical device simulations of crystalline silicon solar cells: a review. *Journal of Computational Electronics*, vol. 10, pp. 314–330, 2011.
13. R. De Rose et al. Open issues for the numerical simulation of silicon solar cells. *IEEE 12th International Conference on Ultimate Integration on Silicon (ULIS)*, pp. 1-4, 2011.
 - A. Fell et al. Input parameters for the simulation of silicon solar cells in 2014. *IEEE Journal of Photovoltaics*, vol. 5, no. 4, pp. 1250–1263, 2015.
14. R. De Rose et al. Understanding the impact of the doping profiles on selective emitter solar cell by two-dimensional numerical simulation. *IEEE Journal of Photovoltaics*, vol. 3, no. 1, pp. 159–167, 2013.